

MULTISCALE RECONSTRUCTION FOR PHOTON-LIMITED SHIFTED EXCITATION RAMAN SPECTROSCOPY

Rebecca Willett

Department of Electrical and Computer Engineering
Duke University, Durham, NC 27708

ABSTRACT

Shifted excitation Raman spectroscopy results in multiple observations of the sum of a material's fluorescent and Raman spectra. The fluorescent spectrum is typically stationary with respect to the excitation frequency induced by the instrument, while the Raman spectrum is subject to a nonlinear shift which depends explicitly and in a known manner upon the excitation frequency. This phenomenon has been exploited to reconstruct Raman spectra indirectly by subtracting spectra observed at two closely spaced excitation frequencies. The technique, known as Shifted Excitation Raman Difference Spectroscopy (SERDS), is of limited utility, however, in that observations with low photon counts are difficult to process accurately, and that one must still reconstruct the spectrum from the estimate of the derivative. This paper presents an innovative alternative approach to Raman spectrum reconstruction based on an expectation-maximization algorithm and multiresolution photon-limited signal analysis. Using this method, it is shown that using multiple excitation frequencies (while keeping the total excitation laser power and total expected photon counts constant) can result in dramatic improvements in reconstruction accuracy.

Index Terms— Poisson processes, Wavelet transforms, Raman spectroscopy, Inverse problems

1. SHIFTED EXCITATION RAMAN SPECTROSCOPY

Raman spectroscopy is widely used to study vibrational modes of molecules in a material; since these modes depend upon the chemical bonds in the material, Raman spectroscopy has enormous potential for material specificity in a broad range of applications [1]. While use of this technology is steadily increasing with the development of cheaper and more efficient photon detectors and laser sources, the effectiveness is impeded by strong fluorescent background spectra which overwhelm the weaker Raman spectra [2]. This key challenge is frequently addressed via shifted excitation Raman spectroscopy (SERS), the process by which the Raman spectrum of a material is estimated using multiple (typically two) noisy observations of the spectrum collected at different (shifted) excitation frequencies. In this context, we may model the in-

tensity of each observed spectrum as the sum of the material's fluorescent spectrum and its Raman spectrum. The fluorescent spectrum is stationary with respect to the excitation frequency induced by the instrument, meaning that every observed spectrum, regardless of excitation frequency, contains noisy observations of the same fluorescent spectrum. This is a result of Kasha's rule, which states that most of the fluorescence is emitted from relaxed vibrational states, so that a small change in excitation frequency does not change the fluorescent spectrum [3]. In contrast, the Raman spectrum is subject to a nonlinear shift which depends explicitly and in a known manner upon the excitation frequency. For more on the physics underlying SERS, see for example [2, 3, 4].

1.1. Problem Formulation

In this paper, the following notation will be used: let ν index frequencies at which spectra are observed, and ν_E an excitation frequency. Denote the fluorescent and Raman spectra as $S_F(\nu)$ and $S_R(\nu)$, respectively, and let

$$S_E(\nu) = A_E (S_F(\nu) + h_E(S_R(\nu))),$$

where A_E is a scalar proportional to the power of the excitation laser (so that higher-powered lasers result in more photon counts) and h_E is the operator which shifts the Raman spectrum in a manner dependent upon the excitation frequency ν_E . For example, we may assume h_E behaves as follows:

$$h_E(S_R(\nu)) = S_R(\nu + c_a\nu_E + c_b\nu\nu_E)$$

for some constants $c_a > 0$ and $c_b \geq 0$. Many researchers, depending upon the specifics of their application, reasonably assume $c_b = 0$, simplifying this expression and the subsequent numerical analysis [2, 3, 4]. The method described in this paper would certainly hold for $c_b = 0$, but we include it in our analysis because the result is then more broadly applicable. Note that the main results of this paper hold for a broad class of functionals h_E , not only the one explored in this paper, and that in general h_E must model the physics of the SERS system.

Consider the discrete spectra defined by integration sam-

The author was partially supported by DARPA, grant no. HR0011-06-1-0026.

pling at the detector array as follows:

$$S_M[n] \equiv \int_{n/N}^{(n+1)/N} S_M(\nu) d\nu$$

$$\mathbf{S}_M = [S_M[0] \cdots S_M[N-1]]^T$$

for $n = 0, \dots, N-1$ and for $M \in \{F, R, E\}$, where the frequency ν has been normalized to lie in the range $[0, 1]$. We then have the following observation model:

$$\mathbf{y}_E \sim \text{Poisson}(\mathbf{S}_E).$$

1.2. Prior Work in SERDS

The phenomenon of fluorescent spectra remaining stationary while Raman spectra shift under different excitation frequencies has been used previously to estimate Raman spectra \mathbf{S}_R . In particular, one common approach is to collect observations under two different excitation frequencies, ν_{E_1} and ν_{E_2} , such that $\nu_{E_1} - \nu_{E_2}$ is small and $A_{E_1} = A_{E_2}$. Note that

$$\begin{aligned} S_{E_1}(\nu) - S_{E_2}(\nu) &= A_{E_1} (h_{E_1}(S_R(\nu)) - h_{E_2}(S_R(\nu))) \\ &= A_{E_1} (S_R(\nu + c_a \nu_{E_1} + c_b \nu \nu_{E_1}) \\ &\quad - S_R(\nu + c_a \nu_{E_2} + c_b \nu \nu_{E_2})) \end{aligned}$$

Thus, the discrete signal $\mathbf{y}_{E_1} - \mathbf{y}_{E_2}$ can be considered a noisy observation of the discrete derivative of \mathbf{S}_R .

For large A_{E_1} (i.e. large photon counts), the observations can be used to estimate this discrete derivative with reasonable accuracy, and from there one can begin to extract important features of the Raman spectrum. Common approaches to estimating \mathbf{S}_R from $\mathbf{y}_{E_1} - \mathbf{y}_{E_2}$ include the following:

- Least-squares fitting of Lorentzian functions to the difference $\mathbf{y}_{E_1} - \mathbf{y}_{E_2}$ [2] – this is a particularly challenging optimization problem when one has no prior knowledge of the locations of the peaks in the true Raman spectrum.
- Numerically integrating the discrete derivative, possibly in conjunction with linear interpolation between the data points [3] – this is only effective in high SNR scenarios.
- Viewing $\mathbf{y}_{E_1} - \mathbf{y}_{E_2}$ as noisy observations of \mathbf{S}_R convolved with $\delta[\cdot] - \delta[\cdot + c_a(\nu_{E_1} - \nu_{E_2})]$, and then performing deconvolution [4] – this is only effective in high SNR scenarios.

1.3. Advantages of the Proposed Approach

In general, most approaches have two key drawbacks: (1) when one wishes to keep A_{E_1} low (for example, when studying the spectra of tissue *in vivo*), the resulting photon-limited observations make accurate estimation of the derivative of S_R and

subsequent inference very challenging, and (2) the methods do not provide a convenient mechanism for estimating S_R using observations from multiple (more than two) excitation frequencies. The innovative method proposed in this paper addresses these challenges by posing the estimation of \mathbf{S}_R as a Poisson inverse problem and using multiscale Poisson intensity estimation methods to yield highly accurate results. It is shown that if K denotes the number of excitation frequencies used, and if the total excitation power is held constant (i.e. $A_{E_1} = A_{E_2} = \cdots = A_{E_K}$ and $\sum_k A_{E_k} = A_\Sigma$), then the reconstruction accuracy remarkably *increases* with K even as the SNR of each observed spectrum *decreases*.

2. POISSON INVERSE PROBLEM FORMULATION

Let \mathbf{y}_k , for $k = 1, \dots, K$, denote the k^{th} N -dimensional observed spectra, resulting from excitation frequency ν_{E_k} and with amplitude $A_{E_k} \equiv A_\Sigma/K$ for some $A_\Sigma > 0$. This results in a total of $N \cdot K$ measurements which can be stacked into a single column vector

$$\mathbf{y} \equiv [\mathbf{y}_1^T \mathbf{y}_2^T \cdots \mathbf{y}_K^T]^T.$$

We can likewise write the spectra \mathbf{S}_R and \mathbf{S}_F as a stacked discrete column vector with $2N$ elements: $\mathbf{S} \equiv [\mathbf{S}_F^T \mathbf{S}_R^T]^T$. Finally, we can write our observation model as

$$\mathbf{y} \sim \text{Poisson}(\mathbf{H}\mathbf{S})$$

where \mathbf{H} in a $NK \times 2N$ matrix which encapsulates the measurement model described Section 1.1.

Using this model, we clearly have a Poisson inverse problem which can be solved using the expectation-maximization (EM) algorithm. In particular, we will use the EM algorithm described in [5], which augments the classical Richardson-Lucy algorithm with Maximum Penalized Likelihood estimation in the M-step. The resulting method consists of iteratively repeating backprojection in the E-step and Poisson denoising in the M-step. Specifically, the E-step consists of a standard Richardson-Lucy iteration:

$$\mathbf{x}^{(t)} = \hat{\mathbf{S}}^{(t)} \cdot \times \left(\mathbf{H}^T \left(\mathbf{y} / \left(\mathbf{H} \hat{\mathbf{S}}^{(t)} \right) \right) \right),$$

where $\cdot \times$ and $\cdot /$ denote element-wise multiplication and division of vectors, respectively. The M-step consists of denoising $\mathbf{x}^{(t)}$ as described in Section 3.

3. MULTISCALE REGULARIZATION

The multiresolution Poisson denoising method of regularization employed in this paper is referred to a TI-Haar tree pruning. Intensity estimates are calculated from noisy realizations in $\mathbf{x}^{(t)}$ by determining the ideal partition of the domain of observations (assumed to be $[0, 1]$ for both the Raman and the fluorescent spectra) and computing the sample average in

each interval of the optimal partition. (We will drop the (t) notation for the remainder of this section.) This approach and its theoretical properties are detailed in [6, 7] and briefly reviewed in this section.

The space of possible partitions is a nested hierarchy defined through a recursive dyadic partition (RDP) of $[0, 1]$, and the optimal partition is selected by pruning a binary tree representation of the observed data. (This binary tree is referred to as a complete RDP.) This gives our estimators the capability of varying the resolution with the frequency ν to automatically increase the smoothing in very regular regions of the spectra and to preserve detailed structure in less regular regions. Pruning decisions are made using a penalized likelihood criterion.

In general, the RDP framework leads to a model selection problem that can be solved by a tree pruning process. Each of the terminal intervals in the pruned RDP could correspond to a region of homogeneous or smoothly varying spectral intensity. Such a partition can be obtained by merging neighboring intervals of (*i.e.* pruning) a complete RDP to form a data-adaptive RDP \mathcal{P} and fitting sample averages to the terminal intervals of \mathcal{P} . Thus the spectrum estimate, $\hat{\mathcal{S}}$, is completely described by \mathcal{P} . Given a partition estimate $\hat{\mathcal{P}}$, $\hat{\mathcal{S}}$ can be calculated by computing the sample average of the observations over each interval in $\hat{\mathcal{P}}$.

This provides for a very simple framework for penalized likelihood estimation, wherein the penalization is based on the complexity of the underlying partition. The goal here is to find the partition which minimizes the penalized likelihood function:

$$\begin{aligned}\hat{\mathcal{P}} &\equiv \arg \min_{\mathcal{P}} \left[-\log p(\mathbf{x} | \mathcal{S}(\hat{\mathcal{P}})) + \text{pen}(\hat{\mathcal{P}}) \right] \\ \hat{\mathcal{S}} &\equiv \mathcal{S}(\hat{\mathcal{P}})\end{aligned}\quad (1)$$

where

$$p(\mathbf{x} | \mathcal{S}(\hat{\mathcal{P}})) = \prod_{i=0}^{N-1} \frac{e^{-S[i]} S[i]^{x[i]}}{x[i]!}$$

denotes the likelihood of observing \mathbf{x} given the spectrum estimate $\mathcal{S}(\hat{\mathcal{P}})$ and where $\text{pen}(\hat{\mathcal{P}})$ is the penalty associated with the estimate $\mathcal{S}(\hat{\mathcal{P}})$. (We penalize the estimates according to a codelength required to uniquely describe each model with a prefix code; the penalties are discussed in detail in [7].) The resulting estimator $\hat{\mathcal{S}}$ is referred to as the maximum penalized likelihood estimator (MPLE).

The accuracy of these estimates can be augmented by a process called cycle-spinning, or averaging over shifts, resulting in translation-invariant (TI) estimates [8]. Cycle-spinning, as originally proposed, requires $O(N \log N)$ operations, but was derived in the context of undecimated wavelet coefficient thresholding in the presence of Gaussian noise, and is difficult to implement efficiently in the case of Poisson noise. The above multiscale tree-pruning method can be modified to produce the same effect by averaging over shifts, but the increase in quality comes at a high computational cost; naïve

algorithms require $O(N^2)$ operations. Novel computational methods, as described in [9], however, can be used to yield TI-Haar tree pruning estimates in $O(N \log N)$ time. Unlike traditional wavelet thresholding techniques, this method is near minimax optimal for Poisson noise distributions and is robust to noise due to the hereditary nature of the tree-pruning process.

4. SIMULATION RESULTS

We have conducted preliminary experiments to demonstrate that one can improve upon SERDS by using multiple excitation frequencies and the Poisson inverse problem framework combined with multiscale regularization as described above. In particular, this simulation experiment holds the *total* excitation laser power $A_{\Sigma} = \sum_k A_{E_k}$ (and hence total expected number of observed photons) constant, so that more excitation frequencies imply more observed spectra, each with a lower SNR.

To generate the experimental data, we set

$$S_F(\nu) = \frac{5\nu^4(1-\nu)^8}{\beta(5,9)} + 0.01$$

where $\beta(\cdot, \cdot)$ is the Beta function, to have the smooth shape of a Beta probability distribution function. The Raman spectrum was a mixture of five Gaussians with random means, variances, and amplitudes. Figure 1 displays a sample set of spectra.

The method was initialized as follows: for each index n , $\hat{\mathcal{S}}_F^{(0)}[n]$ was set to the mean of the $K-1$ *smallest* values of $\mathbf{y}_k[n]$ for $k = 1, \dots, K$ because the largest value could potentially correspond to a peak in the Raman spectrum at the corresponding excitation frequency. To compute $\hat{\mathcal{S}}_R^{(0)}$, we set $\mathbf{z}_k = \mathbf{y}_k - \hat{\mathcal{S}}_F^{(0)}$ to be a rough estimate of the Raman spectrum at each of the K shifts. We then “unshift” each \mathbf{z}_k to produce an estimate of the Raman spectrum at excitation frequency E_1 and set $\hat{\mathcal{S}}_R^{(0)}$ to the average over k . While this method of initialization yielded relatively accurate estimates in the presence of high photon counts, it was less effective for low SNRs, and the ultimate reconstruction accuracy was chiefly due to the efficacy of the proposed Poisson inverse problem framework and multiscale regularization.

For each setting of $K \in \{2, 5, 10, 20, 40\}$ we ran one hundred realizations of the Raman spectrum and the Poisson noise to compute average mean squared errors (MSE). The algorithm terminated the iterations when $\max_n (\hat{\mathcal{S}}_R^{(t)}[n] - \hat{\mathcal{S}}_R^{(t-1)}[n]) \leq 10^{-5}$. The penalty term in (1) was multiplied by a scalar weight to improve empirical performance. The weight was not selected to minimize any particular error metric, but rather to yield generally accurate reconstructions. The below table summarizes the results:

| K | Mean Photon Count per Sample | Average MSE |
|----|------------------------------|-------------|
| 2 | 1000 | 0.159 |
| 5 | 400 | 0.090 |
| 10 | 200 | 0.059 |
| 20 | 100 | 0.053 |
| 40 | 50 | 0.050 |

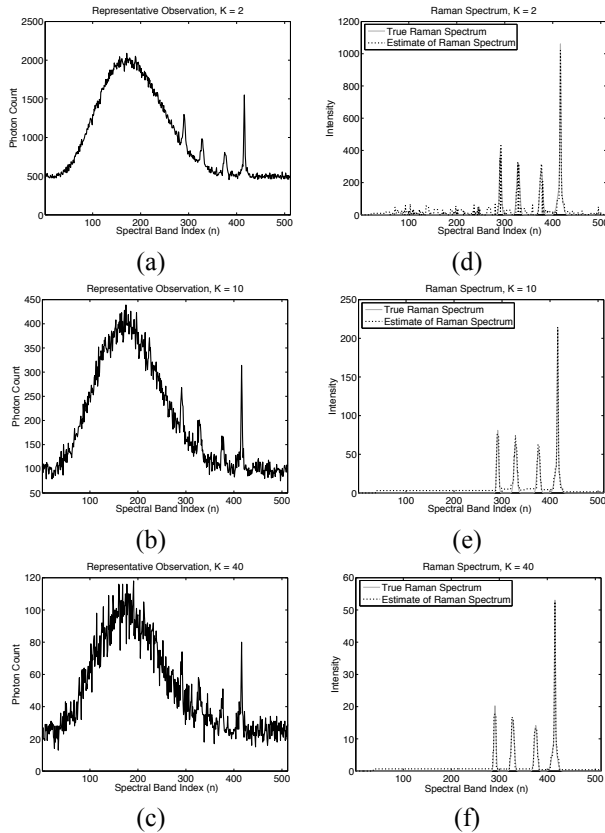


Fig. 1. Experimental results. (a) Representative one of two observed spectra. (b) Representative one of ten observed spectra. (c) Representative one of forty observed spectra. (d) Reconstructed Raman spectrum using two excitation frequencies; MSE = 0.147. (e) Reconstructed Raman spectrum using ten excitation frequencies; MSE = 0.047. (f) Reconstructed Raman spectrum using forty excitation frequencies; MSE = 0.037.

An example result for this experiment is displayed in Figure 1. Clearly the observations are very noisy for $K = 40$, but using the proposed method to exploit the shifting of the Raman spectrum with excitation frequency yielded a significantly better reconstruction than was possible when only using two excitation frequencies (as is the SERDS convention).

5. CONCLUSIONS

This paper demonstrates Shifted Excitation Raman Spectroscopy (SERS) can yield highly accurate reconstructions

when using multiple excitation frequencies. While conventional techniques only use two excitation frequencies and perform reconstruction via a discrete estimate of the Raman spectrum derivative, the method described in this paper poses the reconstruction as a Poisson inverse problem. Combining this framework with multiscale Poisson intensity estimation methods yields accurate reconstructions from very noisy, photon-limited observations using as many as forty different excitation frequencies. Because a significant improvement in accuracy was achieved without an increase in excitation laser power, the proposed method has the potential to advance Raman spectroscopy in a variety of application domains, including biological applications where high laser power could damage the system under study. Preliminary work with real spectroscopic measurements of tissue samples further supports this potential.

While the proposed method has resulted in promising experimental results, several open questions remain to be addressed. These include an investigation into the optimal method of choosing the K excitation frequencies.

6. ACKNOWLEDGMENTS

The author would like to thank Prof. David Brady and Scott McCain of Duke University for their feedback and many helpful discussions.

7. REFERENCES

- [1] J. Ferraro, K. Nakamoto, and C. Brown, *Introductory raman spectroscopy, Second Edition*, Academic press, 2002.
- [2] S. Bell, E. Bourguignon, and A. Dennis, "Analysis of luminescent samples using subtracted shifted raman spectroscopy," *Analyst*, vol. 123, pp. 1729–1734, 1998.
- [3] P. Matousek, M. Towrie, and A. W. Parker, "Simple reconstruction algorithm for shifted excitation raman difference spectroscopy," *Applied Spectroscopy*, vol. 59, 2006.
- [4] J. Zhao, M. Carrabba, and F. Allen, "Automated fluorescence rejection using shifted excitation raman difference spectroscopy," *Applied Spectroscopy*, vol. 56, no. 7, 2002.
- [5] R. Nowak and E. Kolaczyk, "A multiscale statistical framework for Poisson inverse problems," *IEEE Trans. Info. Theory*, vol. 46, pp. 1811–1825, 2000.
- [6] E. Kolaczyk and R. Nowak, "Multiscale likelihood analysis and complexity penalized estimation," *Annals of Stat.*, vol. 32, pp. 500–527, 2004.
- [7] R. Willett and R. Nowak, "Multiscale poisson intensity and density estimation," Submitted to *IEEE Trans. Info. Th.*, 2005.
- [8] M. Lang, H. Guo, J. E. Odegard, C. S. Burrus, and R. O. Wells, "Noise reduction using an undecimated discrete wavelet transform," *IEEE Signal Processing Letters*, vol. 3, no. 1, pp. 10–12, 1996.
- [9] R. Willett and R. Nowak, "Fast multiresolution photon-limited image reconstruction," in *Proc. IEEE Int. Sym. Biomedical Imaging — ISBI '04*, 15-18 April, Arlington, VA, USA, 2004.